0581004

Functional analysis of G protein-coupled receptor GPR56 involved in cortical malformation

（大脳皮質形成異常に関与するGタンパク質共役型受容体GPR56の機能解析）

猪口　徳一
奈良先端科学技術大学院大学
バイオサイエンス研究科　細胞内情報学講座
（伊東　広　教授）

平成２０年5月20日提出

Contents

Abbreviations

NPC: neural progenitor cell

GPCR: G protein coupled receptor

GPS: GPCR proteolytic site

BFPP: bilateral frontoparietal polymicrogyria

SRE: serum-responsive element

NF-κB: nuclear factor-κB

GPR56ECD: GPR56 extracellular domain

p115 RhoGEF RGS: RGS domain of p115 Rho-specific guanine nucleotide exchange factor

mDia1 RBD: RhoA binding domain of mDia1

LPA: L-α-lysophosphatidicacid

GFP: green fluorescent protein

GST: glutathione S-transferase

TRAP6: thrombin receptor-activating peptide 6

MAP: microtubule-associated protein

MAPK: MAP kinase

ERK: extracellular signal-regulated kinase

JNK: c-Jun N-terminal kinase

E: embryonic day

sh: small hairpin

TG2: tissue transglutaminase 2

PEI: polyethyleneimine

Luc: luciferase

TCF: T cell factor

Introduction

In the developing cerebral cortex, neural stem cells divide asymmetrically to generate themselves and neural progenitor cells in the lateral ventricle. Neural progenitor cells (NPCs) then migrate from the ventricular zone to the cortical plate along the radial glial fiber. In this process, called “radial migration,” NPCs terminally differentiate into mature neurons (1). These series of movements are coordinately regulated by various factors, namely, extracellular, cytoskeletal, and signaling molecules (2, 3). Several molecules involved in neuronal cell migration have been identified in studies of cortical development disorders. Reelin, a large protein secreted extracellularly that is associated with the extracellular matrix, controls neuronal positioning work as a terminal signal of radial migration. Mice deficient in Reelin develop an inverted cortex (4–6). Cytoskeleton organization, including the formations of an actin filament and a microtubule, induces the cell shape change and plays a critical role in the regulation of neuronal migration. Two microtubule-associated proteins (MAPs), Lis1 and Dcx, have been shown to be essential for radial migration with the ability to influence microtubule dynamics. The mutation of these two genes results in lissencephaly (7–10). Small GTPases of the Rho family, Rho, Rac, and Cdc42, contribute to cell movement by regulating the actin cytoskeleton (11). The involvement of Lis1 in the regulation of the actin cytoskeleton has been also reported. Lis1 haploinsufficiency resulted in the up-regulation of RhoA activity and a reduction in Rac1 and Cdc42 activities (12). Therefore, the microtubule and actin cytoskeleton coordinately have a crucial role in the regulation of neuronal migration. Although many molecules involved in brain development have been identified, it remains to be clarified how these molecules control NPC behavior by distinct or coordinated signal transduction mechanisms.

G protein-coupled receptors (GPCRs) constitute the largest family of cell surface

receptors and play an important role in controlling key physiological functions, including neurotransmission, hormone release, cell growth, and cell migration (13, 14). Heterotrimeric G proteins transduce signals from GPCRs to an effector (15, 16). Some reports have indicated that G protein signaling is involved in the development of the cerebral cortex by modulating cell migration and proliferation. The γ-aminobutyric acid, type B ($GABA_B$) receptor, which is a member of the GPCR, influences migration from the intermediate zone to the cortical plate during development (17, 18). Stromal cell-derived factor-1 (SDF-1) and its receptor, CXC chemokine receptor 4 (CXCR-4), regulate the tangential migration of interneuron precursors in the developing neocortex. In SDF-1- and CXCR-4-deficient mice, late-generated interneurons fail to integrate into the appropriate neocortical layer (19). Our group showed previously that endothelin-1 (ET-1), a ligand for the endothelin receptor, negatively regulates NPC migration through $G\alpha_q$ and JNK (20). Another group has indicated that the G protein signaling through $G\alpha_{i2}$ maintains mitogenic activity in the NPCs during brain development (21). These studies demonstrated the importance of G protein signaling in the development of the central nervous system.

GPR56 is a newly identified orphan GPCR that belongs to the adhesion GPCR family (22). Adhesion GPCRs have a unique feature in that they contain four highly conserved cysteine residues in a GPCR proteolytic site (GPS) and are thought to function in cell-cell or cell-matrix adhesion because their long N-terminal extracellular regions often contain motifs or domains involved in cell adhesion (23–26). A recent study identified *GPR56* as a cortical development-associated gene. Mutations of *GPR56* cause bilateral frontoparietal polymicrogyria (BFPP) (27). In this disorder, the organization of the frontal cortex is disrupted and shows thinner cortical layers and numerous small folds. Several mutations of *GPR56* with BFPP cause impairment of cell surface expression of the receptor (28). GPR56 mRNA abundantly localizes in the cerebral cortical ventricular and subventricular zones

during periods of neurogenesis, suggesting that GPR56 is expressed in neuronal progenitors (27, 29). It has been reported that the expression level of GPR56 is involved in cancer cell adhesion and metastasis (30–34). However, not only its ligand but also its functions in the developing forebrain and mechanisms of signal transduction remain largely unknown.

To clarify the role of GPR56 in NPC behavior, I first confirmed that GPR56 is highly expressed in NPCs. Next, I analyzed the signaling pathway using the reporter assay and actin reorganization profile. I found that GPR56 activates serum responsive element (SRE)- and nuclear factor-kappa B (NF-κB)-responsive element- mediated transcription through $G\alpha_{12/13}$ and Rho in HEK293T cells. Ectopic expression of GPR56 in NIH3T3 cells induced F-actin accumulation in a $G\alpha_{12/13}$- and Rho-dependent manner. I then found that overexpression of GPR56 inhibited NPC migration. Moreover, the role of endogenous GPR56 on NPC migration was examined using the agonistic antibody against the GPR56 extracellular domain. I demonstrated that GPR56 negatively regulates NPC migration through $G\alpha_{12/13}$ and Rho.

Materials and Methods

Cell Culture, Transfection, and Adenovirus Infection - HEK293T cells and NIH3T3 cells were cultured in Dulbecco's modified Eagle's medium containing 10% fetal bovine serum, 50 μg/ml penicillin, and 50 μg/ml streptomycin. Plasmid DNAs were transfected into cells using the calcium phosphate precipitation method or the Lipofectamine^{TM} 2000 transfection reagent (Invitrogen). For the primary culture of neural progenitor cells, telencephalons of mouse embryo at embryonic day 11.5 (E11.5) were dissected surgically and washed with a buffer containing 124 mM NaCl, 5 mM KCl, 3.2 mM $MgCl_2$, 0.1 mM $CaCl_2$, 26 mM $NaHCO_3$, and 10 mM D-glucose. The dissected telencephalons were treated with 0.05% trypsin for 15 min at 37 °C; this reaction was stopped by adding 70 μg/ml ovomucoid (Sigma). After brief centrifugation, cells were suspended in a Dulbecco's modified Eagle's medium/F12 medium (DF medium; Invitrogen), and 2×10^6 cells were plated in a 100-mm plastic dish coated with 20 μg/ml poly-2-hydroxyethyl methacrylate (poly-HEMA; Sigma). Cells were cultured in DF medium supplemented with B27 (Invitrogen), 20 ng/ml basic fibroblast growth factor, 20 ng/ml epidermal growth factor (Peprotech EC Ltd., London, UK), 1 mg/ml bovine serum albumin, and 2 μg/ml heparin (Sigma) with passage every 2–3 days. All cells were grown in 5% CO_2 at 37 °C. Adenoviruses expressing green fluorescent protein (GFP), GPR56, shGPR56, shCNTRL, C3 exoenzyme, and the RGS domain of the p115 Rho-specific guanine nucleotide exchange factor (p115 RhoGEF RGS) were prepared as described below and previously (35). Neural progenitor cells were infected with adenoviruses at a multiplicity of infection of 0.3–5 for 3 days. Because these adenoviruses express GFP, the infection of adenoviruses can be monitored by GFP fluorescence.

Plasmid Constructs and Adenovirus Preparation - Mouse GPR56 and

transglutaminase 2 (TG2) cDNAs were obtained from the American Type Culture Collection (IMAGE clone ID 3709247 and ID 3256943 respectively). For pCMV5-GPR56, the cDNA of GPR56 was amplified by PCR with primers 5′-GAAGATCTATGGCTGTCCAGGTGCTGC-3′ and 5′-ACGCGTCGACTTAGATGCGGCTGGAGGAGGTG-3′. The PCR product was cloned into the BglII/SalI sites of pCMV5. For pFastBac-GPR56ECD-His, cDNA was amplified by PCR from pCMV5-GPR56 with primers 5′-GAAGATCTATGGCTGTCCAGGTGCTGC-3′ and 5′-GAAGATCTCTAGTGATGGTGATGGTGATGGAGGTAGTGTTTGTGAGTGG-3′ and cloned into the BglII site of pFastBac1. For pFastBac1-GST-TG2, the cDNA of TG2 was amplified by PCR with primers 5′-GCTCTAGAATGGCAGAGGAGCTGCTC-3′ and 5′-GCTCTAGATTAGGCCGGGCCGATGAT-3′. The PCR product was cloned into the XbaI site of pFastBac1-GST. BFPP-associated mutants of GPR56, GPR56 (R38W, Y88C, C91S, C346S, R559W) were made by site directed mutagenesis using pCMV5-GPR56 as a template. The DNAs of $G\alpha_{13}$ (Q226L) and the RGS domain (including residues 1–252) of p115 RhoGEF were amplified by PCR and subcloned into the pCMV5-FLAG vector. pCMV5-Myc-βARK-ct, pEF-Bos-C3, pCMV5-$G\alpha_{13}$ (Q226L), pCMV5-FLAG-RhoA, pCMV5-FLAG-RhoA (G14V), pCMV5-FLAG-RhoA (T19N), pCMV5-FLAG-Rac1 (T17N), and pCMV5-FLAG-Cdc42 (T17N) were prepared as described previously (36). The *Escherichia coli* expression plasmid encoding the RhoA binding domain (RBD) of mDia1 was constructed and introduced into *E. coli* BL21 CodonPlus (DE3)-RIL as described previously (37). GSTmDia1RBD was expressed and used for a pulldown assay. The adenovirus expressing GPR56 was made using the AdEasy XL adenoviral vector system (Stratagene, La Jolla, CA). Briefly, GPR56 cDNA was subcloned into the BglII/SalI sites of the pShuttle-IRES-hrGFP-1 shuttle vector from pCMV5-GPR56. The adenoviruses expressing GFP, p115 RhoGEF RGS, and the C3 exoenzyme were kindly provided by Dr. H.

Kurose (Kyushyu University). The oligonucleotide sequences used in the construction of the small interference RNA vector were as follows: shGPR56, 5′-CGCGTCCGGTAGAAGCCACTCACAAATTCAAGAGATTTGTGAGTGGCTTCTAC CTTTTTA-3′ and 5′-AGCTTAAAAAGGTAGAAGCCACTCACAAATCTCTTGAATTTGTGAGTGGCTTC TACCGGA-3′; shCNTRL, 5′-CGCGTCCAAATGTACTGCGTGGAGACTTCAAGAGAGTCTCCACGCAGTACATT TTTTTTA-3′ and 5′-AGCTTAAAAAAAATGTACTGCGTGGAGACTCTCTTGAAGTCTCCACGCAGTAC ATTTGGA-3′. The oligonucleotides were annealed and then ligated into MluI/HindIII sites of the pRNAT-H1.1/Adeno vector (GenScript, Edison, NJ). These plasmids were introduced into BJ5183-AD-1-competent cells carrying the pAdEasy1 vector. The recombinant adenoviral plasmid was digested with PacI and transfected into HEK293 cells, where virus particles were produced.

TG2, GPR56ECD and Antibodies – Mouse TG2 was generated using a baculovirus-Sf9 expression system and purified with glutathione Sepharose. GST-tag was cleaved and removed using a PreScission Protease. Purified TG2 was dialyzed with TBS. Mouse GPR56ECD was generated using a baculovirus-Sf9 expression system and purified with ion exchange chromatography and affinity chromatography for His-tagged proteins as described previously (38). Briefly, a pFast-Bac-1 vector containing GPR56ECD was introduced into DH10Bac. The recombinant bacmid was prepared to be transfected into Sf9 cells. Recombinant baculovirus-infected Sf9 cells were cultured for 72 h, and the supernatant of the culture medium was applied to SP-Sepharose FF column chromatography. Elution with 50 mM sodium phosphate, pH 8.0, 500 mM NaCl, and 10 mM imidazole was collected and used for nickel-nitrilotriacetic acid-agarose. GPR56ECD was eluted with 400

mM imidazole and dialyzed against 50 mM sodium phosphate, pH 8.0. A Mono-S column was used for the final purification step. The rabbit polyclonal GPR56 antibody was generated against the recombinant GPR56ECD. The antibody was affinity-purified from the antiserum using a GPR56ECD-conjugated column and dialyzed with PBS. The control antibody used in this study was prepared using mouse Asef2 as the antigen and affinity-purified following the same method. A mouse monoclonal antibody Rat401 against nestin was obtained from BD Biosciences. A mouse monoclonal antibody TUJ1 against βIII-tubulin was obtained from Babco (Richmond, CA). A mouse monoclonal antibody M2 against FLAG-peptide was obtained from Sigma. A mouse monoclonal antibody C4 against actin was obtained from Chemicon International (Temecula, CA). Antibody against p38 was obtained from Santa Cruz Biotechnology (Santa Cruz, CA). Antibodies against p44/42 MAPK, phospho-p44/42 MAPK, phospho-p38, and JNK were obtained from Cell Signaling Technology (Danvers, MA). Antibody against phospho-JNK was obtained from Promega (Madison, WI). Antibody against TG2 was obtained from LAB BISION (Fremont, CA). Anti-mouse and anti-rabbit IgG antibodies conjugated with horseradish peroxidase were obtained from GE Healthcare. Alexa-594 phalloidin, Alexa-488-conjugated anti-rabbit IgG, and Alexa-594- and Alexa-350-conjugated anti-mouse IgG were obtained from Molecular Probes, Inc. (Eugene, OR).

Immunoblotting - Samples in a Laemmli buffer were separated using SDS-polyacrylamide gels. The separated proteins were transferred to polyvinylidene difluoride membranes. After blocking for more than 30 min in 5% skim milk-TBST (50 mM Tris-HCl, pH 7.4, 150 mM NaCl, 0.1% Tween 20), membranes were probed for 1 h with primary antibodies in 5% skim milk-TBST. The membranes were then washed three times with TBST and incubated with secondary antibodies coupled to horseradish peroxidase. Immunoblotting was visualized by using an enhanced chemiluminescence

Western blotting detection kit (GE Healthcare).

Immunocytochemistry and Immunohistochemistry - NIH3T3 cells were plated onto 13-mm poly-D-lysine-coated coverslips. Two days later, cells were serum-starved for 6 h. Neural progenitor cells were cultured on the polyethyleneimine (PEI)/ laminin-coated coverslips with basic fibroblast growth factor for 3 days. Cells were fixed in 4% paraformaldehyde in PBS for 30 min, washed three times with PBS for 10 min each, blocked for 30 min with a blocking solution (10% fetal bovine serum and 0.1% Triton X-100 in PBS for NIH3T3 cells or 10% fetal bovine serum in PBS for NPCs), and incubated with primary antibodies for 1 h. Coverslips were incubated with the appropriate secondary antibodies or Alexa-594 phalloidin for 30 min. For immunohistochemistry, E16.5 mouse brain was dissected, fixed overnight in 4% paraformaldehyde in PBS at 4 °C, and impregnated with 30% sucrose in PBS. Cryosections were cut at a thickness of 30 μm and immunostained with primary antibodies in a blocking solution overnight and with secondary antibodies in PBS overnight. The concentrations of antibodies and dye used were: anti-FLAG antibody, 1 μg/ml; anti-GPR56 antibody, 0.4 μg/ml; anti-nestin antibody, 1 μg/ml; anti- III-tubulin, 1 μg/ml; Alexa-488-conjugated anti-rabbit IgG and Alexa- 350- and Alexa-594-conjugated anti-mouse IgG, 2 μg/ml; and Alexa-594 phalloidin, 2 units/ml. Samples were mounted and photographed with a Zeiss Axiophoto fluorescence microscope. A confocal image of NPCs was captured by a Zeiss LSM510 and analyzed.

Reporter Gene Assay - HEK293T cells were seeded in a 48-well plate with about 70% confluence. Cells were transfected with 30 ng/well firefly luciferase reporter gene plasmids (SRE-Luc, SIE-Luc, CRE-Luc, c-fos-Luc, AP1-Luc, NF-κB-Luc, TCF-Luc, and SRF-Luc) and 0.6 ng/well Renilla-luciferase (Renilla-Luc) plasmid in combinations with other plasmids. For some experiments, cells were treated with 1 μg/ml pertussis toxin (Funakoshi Chemical Ltd., Tokyo, Japan) or a 10 μM $G\alpha_{q/11}$ inhibitor YM-254890 (39) 1 h

after transfection. Anti-GPR56 antibody and GPR56ECD were added 6 h before harvesting the cells. Twenty-four hours after transfection, the cells were resuspended in a passive lysis buffer, and the luciferase activity was then measured with a luminometer (ARVO MX, PerkinElmer Life Sciences) using the Dual-Luciferase reporter assay system (Promega, Madison, WI). Firefly luciferase activity was normalized to the internal control activity of Renilla-luciferase.

Pulldown Assays – For pulldown assay of Rho-GTP, HEK293T cells were transfected with pCMV5-FLAG-RhoA (wild type, G14V, T19N) with or without pCMV5-GPR56. Thirty-six hours after serum starvation, the cells were stimulated with or without 15 μg/ml anti-GPR56 antibody for 10 min and lysed in 300 μl of lysis buffer A (20 mM HEPES-NaOH, pH 7.5, 150 mM NaCl, 20 mM MgCl2, 0.5% Nonidet P-40, 1 μg/ml leupeptin) per-35mm dish. After centrifugation at 15,000 × g at 4 °C for 10 min, 200 μl of supernatant was incubated with 25 μg of GST-mDia1RBD and glutathione-Sepharose at 4 °C for 30 min. The resins were washed twice with lysis buffer A and boiled in Laemmli sample buffer. Eluted samples were subjected to SDS-PAGE. Bound RhoA was detected by immunoblotting using an anti-FLAG antibody. For pulldown assay of TG2, recombinant TG2 (50 nM) was incubated with hexahistidine-tagged GPR56ECD (100 nM) which was immobilized to Ni-NTA agarose in a binding buffer (20 mM Tris-HCl, pH7.5, 150 mM NaCl, 0.5% Nonidet P-40) with various concentrations of $CaCl_2$ (0, 1, 5, 10 and 20 mM) at 4 °C for 2.5 h, forrowed by washing three times with a binding buffer. TG2 and GPR56ECD were detected by immunoblotting.

MAP Kinase Assays - HEK293T cells were transfected with or without pCMV5-GPR56. Thirty-six hours after serum starvation, the cells were stimulated with 15 μg/ml anti-GPR56 antibody for 3, 10, and 20 min, 1 μM lysophosphatidic acid (LPA) for 20 min, or 10 μM thrombin receptor-activating peptide 6 (TRAP6) for 20 min. Cell lysates

were prepared with the lysis buffer B (20 mM HEPES-NaOH, pH 7.5, 100 mM NaCl, 3 mM MgCl2, 1 mM dithiothreitol, 1 mM phenylmethanesulfonyl fluoride, 1 mM EGTA, 1 mM Na_3VO_4, 10 mM NaF, 10 mM β-glycerophosphate, 0.5% Nonidet P-40, 1 μg/ml leupeptin). After sonication and centrifugation at 15,000 × g at 4 °C for 10 min, the supernatants were subjected to SDS-PAGE. Activation of MAPKs (ERK, JNK, and p38) was assessed by immunoblotting using each anti-phospho-MAPK antibody.

Measurement of Intracellular Ca^{2+} Mobilization - Intracellular calcium mobilization was measured using the fluorescent Ca^{2+} indicator Fura-2 acetoxymethyl ester (Fura-2/AM) (Dojin Kagaku). Briefly, HEK293T cells were washed, detached in a suspension buffer (20 mM HEPES-NaOH, pH 7.5, 140 mM NaCl, 5.4 mM KCl, 1.8 mM $CaCl_2$, 0.8 mM $MgCl_2$, and 5.6 mM glucose). The suspended cells were loaded with 2 μM Fura- 2/AM for 30 min at 30 °C and then washed with a suspension buffer to remove the extracellular dye. For the fluorimetric measurement, 1×10^6 cells were placed into a cuvette in a thermostatically controlled cell holder at 37 °C with continuous stirring. The cells were stimulated with 1 μM LPA or 7.5 μg/ml anti-GPR56 antibody. Fluorescence was monitored using an F-2000 fluorescence spectrophotometer (Hitachi) with emission at 510 nm after excitation at 340 and 380 nm.

Migration Assay - The migration assay was performed as described previously (20) with slight modifications. The migration of neural progenitor cells was performed in a 96-well dish precoated with PEI. The 96-well dish was coated with 50 μl of 0.1% PEI in a 30 mM boric acid buffer (pH 8.4) for at least 6 h at room temperature and washed three times with distilled water. Eighty μl of a differentiation medium (a DF medium with B27, 1 mg/ml bovine serum albumin) was added to a well, and 20 μl of a 3 day-cultured neurospheres suspension (including 20–40 neurospheres) was then added to the well. Twenty-four hours later, the number of migrating neurospheres was counted. Migration was

assessed by measurement of the distance from the edge of the neurosphere to the leading cell of outgrowth. If this distance was more than the diameter of the neurosphere or the neurosphere was completely dispersed, this sphere was evaluated as a migrating neurosphere. The migration activity was indicated by the ratio of migrating neurospheres to total neurospheres.

Results

GPR56 Is Highly Expressed in Neural Progenitor Cell Membranes as a Cleaved Form - To analyze the tissue-specific distribution and developmental expression of GPR56, a polyclonal antibody against the baculovirus-expressed N-terminal extracellular region of GPR56 was generated and used it for immunoblotting and immunocytochemistry. It has been reported that the N-terminal extracellular region of GPR56 is cleaved at the GPS motif during processing (32). Thus, the anti-GPR56 antibody recognized both the full-length GPR56 (GPR56FL) at 75 kDa and the cleaved extracellular domain of GPR56 (GPR56ECD) at 62 kDa (Fig. 1, A and B). GPR56 was highly expressed mainly as the cleaved form in NPCs. In mouse brain, cleaved GPR56 expression was high from E13 to postnatal day 7 but significantly low in adulthood. On the other hand, GPR56FL was observed in the late stage of development with a lower expression level (Fig. 1A). In adult tissues, GPR56 was ubiquitously expressed mainly as the noncleaved GPR56 (Fig. 1B). Immunocytochemical analysis using confocal laser scanning microscopy indicated the membrane surface expression of GPR56 in NPCs (Fig. 1C). To confirm the expression of GPR56 in NPCs in vivo, I performed immunohistochemical staining using E16.5 mouse brain slices. As shown in Fig. 1D, GPR56 expression was detected in the ventricular and subventricular zones, as observed with the antibody against nestin, which is an NPC marker. The expression of βIII-tubulin, which is a neuron- specific marker, was different from that of GPR56. These results were consistent with previous reports that GPR56 mRNA is specifically expressed in the ventricular zone of the mouse cerebral cortex in the early stage of development and in the adult hippocampus, where it contains NPCs and maintains neurogenesis.

GPR56 Signal Negatively Regulates NPC Migration - A recent study indicated that

the mutation of GPR56 is involved in cortical malformation (27). Cortical malformations have been thought to be caused by the impairment of migration of NPCs at the developmental process of the cerebrum. My study showed a cell surface expression of GPR56 in the NPCs. Next, I investigated whether the GPR56 signal can regulate NPC migration. Our group previously developed an assay system to evaluate the migration of NPCs *in vitro* (20). Using this migration assay system with the neurospheres, I assessed the migrating activity of NPCs. Neuronal progenitor cells were infected with the recombinant adenovirus harboring the GFP or GPR56 gene at a multiplicity of infection of 0.3–5 and cultured for 3 days. Expression of GPR56 and GFP in NPCs was assessed by immunoblotting (Fig. 2A). Neurospheres were put on polyethyleneimine- coated dishes. Twenty-four hours after plating, NPCs moved out from the noninfected and control GFP adenovirusinfected neurospheres. Remarkably, GPR56 overexpression decreased the migration of NPCs from neurospheres in an expression level-dependent manner (Fig. 2, B and C). GPR56-overexpressing cells took a round shape in the neurosphere. These results suggest that the GPR56 signal negatively regulates NPC migration.

GPR56 Stimulates SRE- and NF-κB-responsive Element-mediated Transcription through $G\alpha_{12/13}$ and Rho - Seifert and Wenzel-Seifert (40) have reported that the overexpression of GPCR can induce signal activation in a ligand-independent manner. To investigate the signaling pathways of GPR56, I examined the effect of GPR56 overexpression on luciferase reporter genes with various transcriptional elements. Each reporter gene was transfected into HEK293T cells with or without GPR56 expression plasmid, and the luciferase activity was measured. In the cells transfected with GPR56, the transcriptional activity of the SRE- and NF-κB-responsive element was increased up to 3–4 fold. Slight increases of CRE- and SRF mediated luciferase activities were detected. However, the transcriptional activity of other elements was not affected by GPR56

overexpression (Fig. 3A). It has been reported that $G\alpha_{i/o}$, $G\alpha_{q/11}$, $G\alpha_{12/13}$, and $G\beta\gamma$ activate SRE-dependent transcriptional activity under GPCR stimulation. Therefore, I investigated which $G\alpha$ isoforms or $\beta\gamma$ subunits act downstream of GPR56 using inhibitory molecules for these subunits. The SRE-luciferase reporter gene and GPR56 cDNA were transiently transfected with FLAG-p115 RhoGEF RGS and Myc-βARK-ct, which inhibit $G\alpha_{12/13}$ and $G\beta\gamma$, respectively. Pertussis toxin and YM-254890, which are specific inhibitors of $G\alpha_{i/o}$ and $G\alpha_{q/11}$, respectively, were utilized from 1 h after transfection. FLAG-p115 RhoGEF RGS completely suppressed the GPR56- induced SRE-luciferase activity (Fig. 3B), suggesting that GPR56 couples with $G\alpha_{12/13}$. However, pertussis toxin and YM-254890 failed to suppress. It is known that $G\alpha_{12/13}$ activates Rho through the Rho-specific guanine nucleotide exchange factor and that Rho induces SRE-mediated transcriptional activation. To confirm the involvement of Rho, I examined the effect of botulinum C3 exoenzyme and the dominant negative mutants of RhoA, Rac1, and Cdc42. The C3 exoenzyme and the RhoA dominant negative mutant inhibited SRE- mediated transcriptional activation by GPR56, whereas the dominant negative mutants of Rac1 and Cdc42 did not (Fig. 3C). The activation of NF-κB-responsive element-mediated luciferase activity was also inhibited by p115 RhoGEF RGS, the C3 exoenzyme, and the RhoA dominant negative mutant in the same manner (data not shown). These results suggested that GPR56 couples with $G\alpha_{12/13}$ and activates SRE- and NF-κB- mediated transcription in a Rho-dependent manner.

GPR56 Induces F-actin Accumulation in NIH3T3 Cells - Rho family small GTPases play a central role in the regulation of the actin fiber reorganization. It has been reported that the overexpression of some GPCRs that couple with $G\alpha_{12/13}$ can induce actin fiber reorganization (41). Therefore, I examined whether GPR56 has the ability to induce actin fiber reorganization. First, I attempted to examine the effect of GPR56 overexpression in NPCs. Although weak F-actin accumulation at the cell periphery was observed, it was

difficult to detect the actin stress fiber formation (data not shown). Therefore, I used NIH3T3 fibroblast cells. Overexpression of GPR56 induced the formation of F-actin in NIH3T3 cells. Actin fiber reorganization was similarly observed in cells expressing active mutants of $G\alpha_{12/13}$ and RhoA but not in control GFP (Fig. 4A). To confirm the involvement of $G\alpha_{12/13}$ and Rho activation in GPR56-induced actin reorganization, GPR56 was co-transfected with p115 RhoGEF RGS or dominant negative mutants of Rho family small GTPase. In NIH3T3 cells, p115 RhoGEF RGS and the RhoA dominant negative mutant inhibited GPR56-induced F-actin formation (Fig. 4B). These results suggest that GPR56 signaling leads to Rho-dependent actin reorganization.

Anti-GPR56 Antibody Has an Agonistic Activity and Induces GPR56-dependent Rho Activation - Previous studies have demonstrated that some antibodies against cell surface receptors act as functional antibodies (42–44). Therefore, I examined the possibility that the anti-GPR56 polyclonal antibody has a functional activity through GPR56. HEK293T cells were transfected with the GPR56 expression plasmid and the SRE-luciferase gene and treated with the indicated amounts of the anti-GPR56 antibody. In this experiment, I used a small amount of the GPR56 expression plasmid to assess the effect of the anti-GPR56 antibody. The SRE-luciferase activity of mock-transfected cells was not affected by the anti-GPR56 antibody treatment. In the case of GPR56-transfected cells, the anti-GPR56 antibody, but not the control antibody, stimulated luciferase activity in a dose-dependent manner (Fig. 5A). Moreover, this positive effect of the anti-GPR56 antibody on the luciferase activity was attenuated by neutralizing the antibody with an antigen, the extracellular domain of GPR56. These results indicated that the anti-GPR56 antibody against its extracellular domain has the ability to induce transcriptional activation through GPR56 as a ligand. To confirm whether GPR56 activates Rho, I performed the pulldown assay using GST-mDia1RBD. As shown in Fig. 5B, transfection of GPR56 slightly

increased GTP-bound form of RhoA. Furthermore, the anti-GPR56 antibody remarkably increased GTP-bound form of RhoA in GPR56-transfected cells, but not in mock-transfected cells. It is known that some GPCRs couple to multiple G proteins. To investigate whether GPR56 stimulates not only $G\alpha_{12/13}$ but also $G\alpha_{i/o}$ and/or $G\alpha_{q/11}$, I examined the activation of MAP kinases and intracellular calcium mobilization. As shown in Fig. 5C, the overexpression of GPR56 did not activate ERK, JNK, or p38. Anti-GPR56 antibody did not affect these activations in GPR56-transfected cells, whereas LPA and TRAP6, in which receptors couple to $G\alpha_{i/o}$, $G\alpha_{q/11}$, or $G\alpha_{12/13}$, activated ERK and JNK. Furthermore, LPA induced calcium response remarkably, whereas the anti-GPR56 antibody did not induce calcium response in GPR56-transfected cells as compared with the response in mock-transfected cells (Fig. 5D). These results suggest that GPR56 transmits a signal mainly to $G\alpha_{12/13}$ but not to $G\alpha_{i/o}$ or $G\alpha_{q/11}$.

Inhibition of NPC Migration by Anti-GPR56 Antibody Requires GPR56 Expression - Next, I examined the effect of the anti-GPR56 antibody on the migration of NPCs. The migration assay was performed with an anti-GPR56 antibody or a control antibody. As in the case of GPR56 overexpression, anti-GPR56 antibody inhibited NPC migration. This effect of the anti-GPR56 antibody was also attenuated by the addition of GPR56-ECD (Fig. 6, A and B). These data indicated that the anti-GPR56 antibody acts on endogenous GPR56 expressed in NPCs. Next, GPR56 knockdown experiments were performed with an adenovirus expressing small hairpin RNA for GPR56 (shGPR56). As shown in Fig. 6C, infection with the adenovirus of shGPR56 decreased the GPR56 expression in NPCs. Although the knockdown of GPR56 did not affect cell migration, anti-GPR56 antibody-induced inhibition was canceled with shGPR56 adenovirus infection (Fig. 6, D and E).

GPR56 Signal Negatively Regulates NPC Migration through $G\alpha_{12/13}$ and Rho -

Because GPR56 overexpression induced the transcriptional activation in HEK293T cells and actin reorganization in NIH3T3 cells through $G\alpha_{12/13}$ and Rho, I investigated the involvement of $G\alpha_{12/13}$ and Rho in the anti-GPR56 antibody-induced inhibition of NPC migration. The inhibitory effect of the anti-GPR56 antibody on NPC migration was completely blocked by infection with an adenovirus expressing p115 RhoGEF RGS or the C3 exoenzyme. In contrast, a specific $G\alpha_q$ inhibitor, YM-254890, did not attenuate the effect of the anti- GPR56 antibody (Fig. 7). Collectively, these data indicate that GPR56 negatively regulates NPC migration through $G\alpha_{12/13}$ and Rho.

BFPP-associated Mutations of GPR56 Affect Post-translational Modification and Cell Surface Expression – In the BFPP patients, five types of single amino acid mutations of GPR56 were reported (27). To investigate the BFPP-associated mutations on GPR56 function, I made these GPR56 mutants, R38W, Y88C, C91S, C346S, and R559W. Each mutant was trasfected into HEK293T cells and subjected to immunoblotting. GPR56ECD and GPR56Full were detected in the GPR56WT transfected cells (Fig. 8A). On the other hands, low molecular weight band of GPR56ECD (Fig. 8A, *lower arrowhead*) was detected in the cells transfected with GPR56 mutants, R38W, Y88C, C91S, and R559W. GPR56 is known to be highly glycosylated (28). This band shift to low molecular weight may be caused by aberrant glycosylation. Interestingly in the cells transfected with C346S, band of GPR56ECD was not detected. In all of the cells transfected with BFPP mutants, high molecular weight band of GPR56Full (Fig. 8A, *upper arrow*), which may be unfolded protein, was detected. Next, to reveal the proper translocation of receptors to the cell surface, each mutant transfected cells were immunostained under non-permeabilized or permeabilized condition. GPR56WT was expressed on the cell surface, but GPR56 mutants were rarely detected on the cell surface, in spite of same level expression of each receptor in the cells (Fig. 8B). These results indicated that BFPP-associated mutation of GPR56 affect

expression of functional receptor on the cell surface.

TG2 Directly Binds to GPR56ECD in a Calcium-Dependent Manner. – Xu *et al*. (32) reported that transglutaminase 2 (TG2) binds to GPR56 ECD. Therefore, I next, examined whether TG2 would be a ligand for GPR56. I previously detected the endogenous TG2 which was immunoprecipitated with transiently expressed full length GPR56, but it was not clear whether the binding between TG2 and GPR56 is direct or not. To confirm direct binding between TG2 and GPR56ECD, pulldown assay was performed with recombinant proteins. Recombinant TG2 was expressed and purified by baculovirus expression system as described in the materials and methods. Recombinant TG2 (50nM) was pulled down by hexahistidine-tagged GPR56ECD (100nM) which was immobilized to Ni-NTA agarose. TG2 is known to be activated its transglutaminase activity in a Ca^{2+}-dependent manner. Therefore, pulldown assay was performed with various concentrations of $CaCl_2$ (0, 1, 5, 10 and 20 mM). TG2 and GPR56ECD were detected by immunoblotting. In the absence of calcium, no significant difference in TG2 binding was detected between control and sample with GPR56ECD. However, TG2 was pulled down with GPR56ECD in a Ca^{2+}-dose dependent manner. Interestingly, GPR56ECD was also detected as high molecular bands, which may be closslinked by TG2. These results suggest that GPR56ECD binds to TG2 and is subjected to some modification in a calcium dependent manner. Next, I investigated the effect of coexpression of TG2 on the GPR56-induced transcriptional activation using SRE-luciferase. However, the coexpression of TG2 did not show any effect on the SRE-mediated transcription (data not shown).

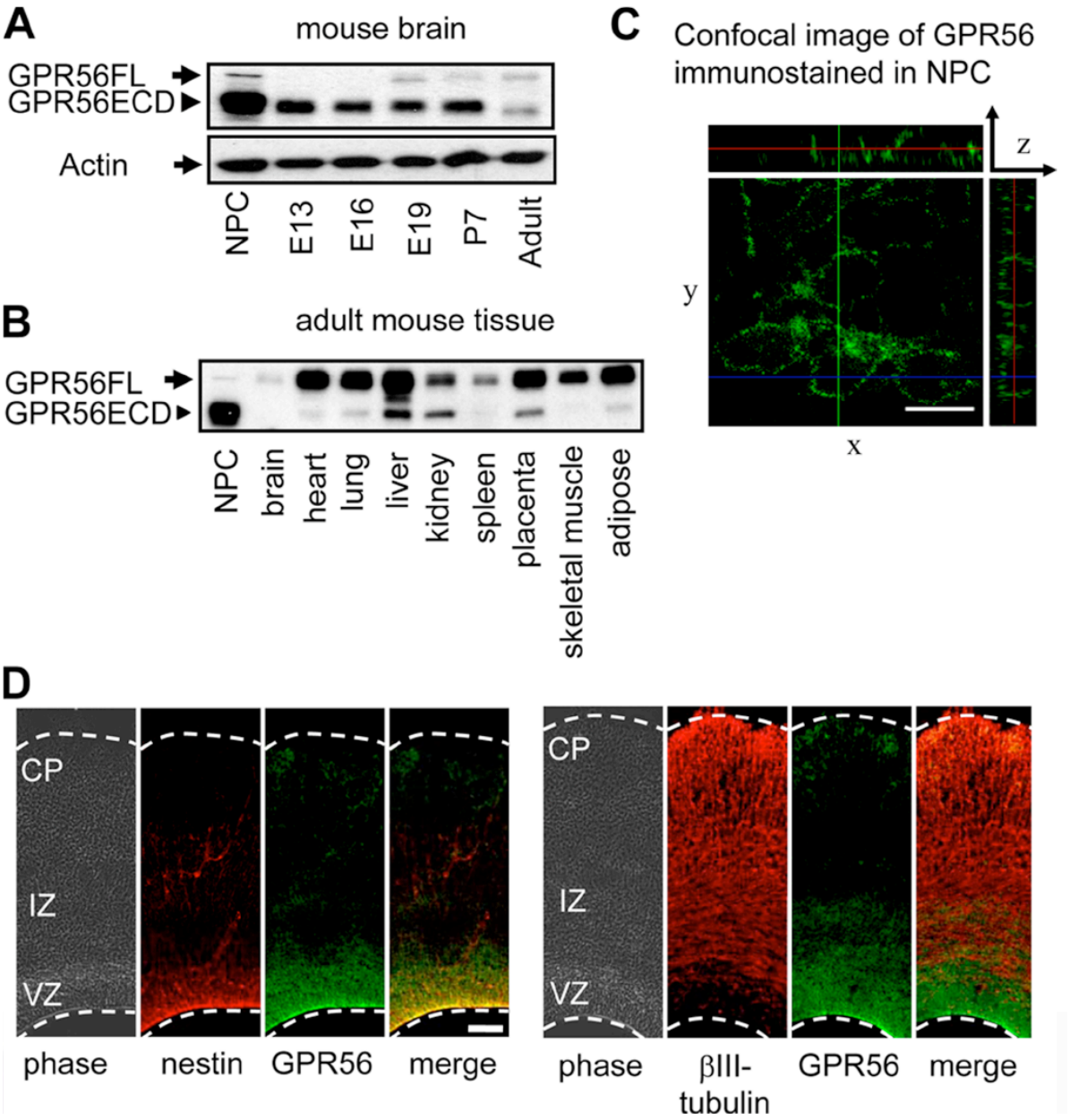

FIGURE 1. **GPR56 is highly expressed in neural progenitor cell membranes as a cleaved form.** (A) Immunoblotting analysis of GPR56 in mouse brain at various developmental stages and in NPCs. Full-length GPR56 (*upper arrow*) and GPR56ECD (*arrowhead*) that is cleaved in the GPS domain are shown. (B) Immunoblotting analysis of GPR56 in adult mouse tissues and NPCs. (C) Immunofluorescent localization of endogenous GPR56 in NPC. NPCs were cultured on PEI/laminin-coated coverglasses with basic fibroblast growth factor for 3 days. Then, cells were fixed and immunostained with anti-GPR56 antibody and visualized by confocal microscopy. The upper panel is an x-z image of the vertical section, the lower left panel is an x-y image of the horizontal section, and the lower right panel is a y-z image of the vertical section. *Bar*, 10 μm. (D) Immunohistochemical staining of E16.5 mouse forebrain with the anti-GPR56 antibody. Cortical slices were prepared from E16.5 mouse telencepharon. Slices were fixed and immunostained with antibodies against nestin, GPR56, and βIII-tubulin. The cortical plate (*CP*), intermediate zone (*IZ*), and ventricular zone (*VZ*) in the cortical region are shown. *Bar,* 100 μm.

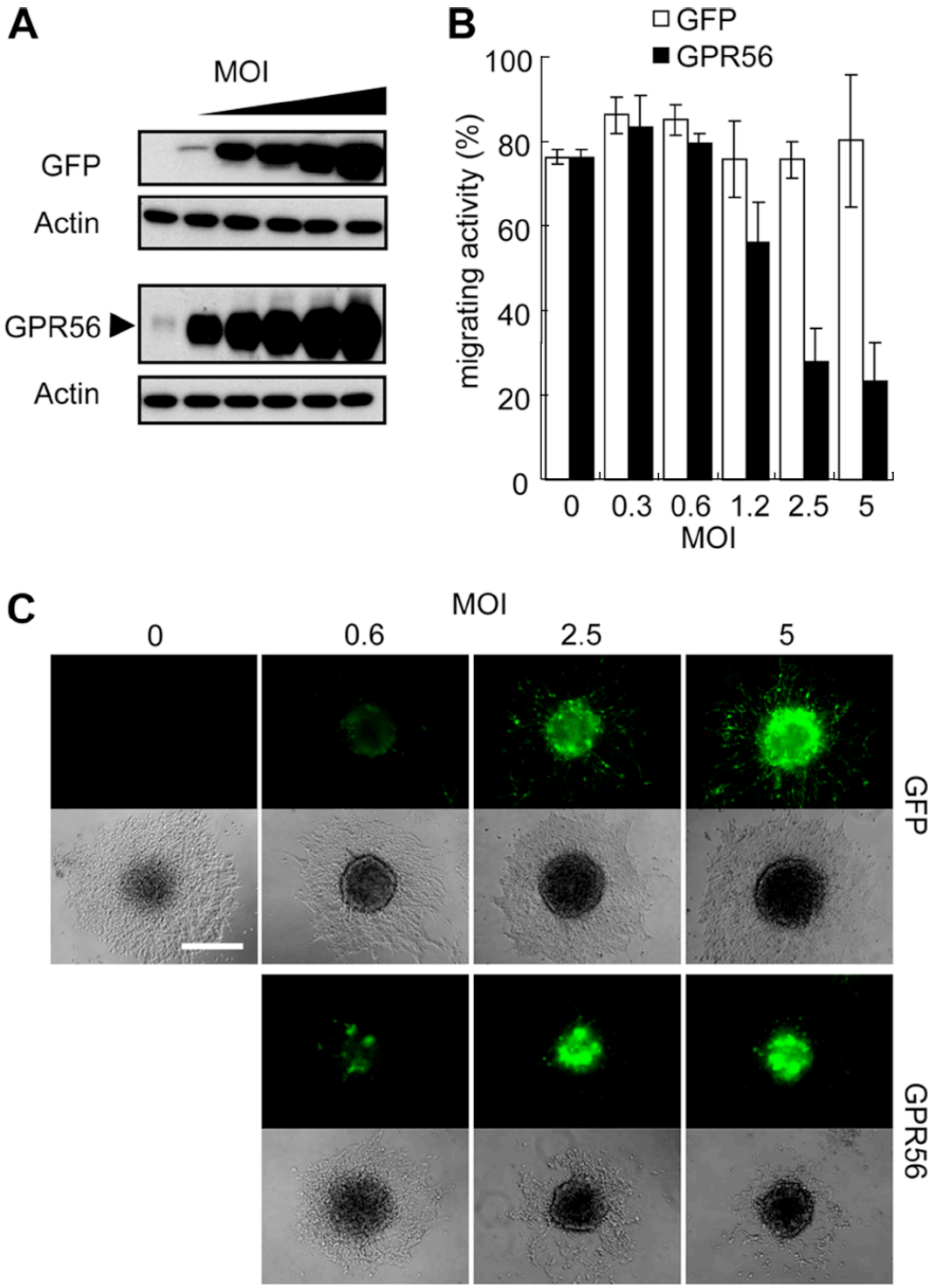

FIGURE 2. **Overexpression of GPR56 negatively regulates NPC migration.** Neural progenitor cells were infected with an adenovirus harboring GFP, GPR56, at a multiplicity of infection (MOI) of 0.3–5 and cultured under undifferentiated conditions to generate the neurosphere. (A) Expression of GPR56, GFP, and actin in adenovirus-infected NPCs was detected by immunoblotting. (B) 72 h after infection, neurospheres were plated on a 96-well plate coated with PEI. Plated neurospheres were cultured for 24 h in a differentiation medium. The effect of GPR56 overexpression on the migration of NPCs was quantitated as a percentage of the migrating neurospheres (*error bars*, ±S.D.). (C) Representative phase-contrast images and GFP-positive adenovirus-infected cells are shown. The data shown are the average of triplicate samples (B) and are representative (A and C) of at least three separate experiments. *Bar*, 250 μm.

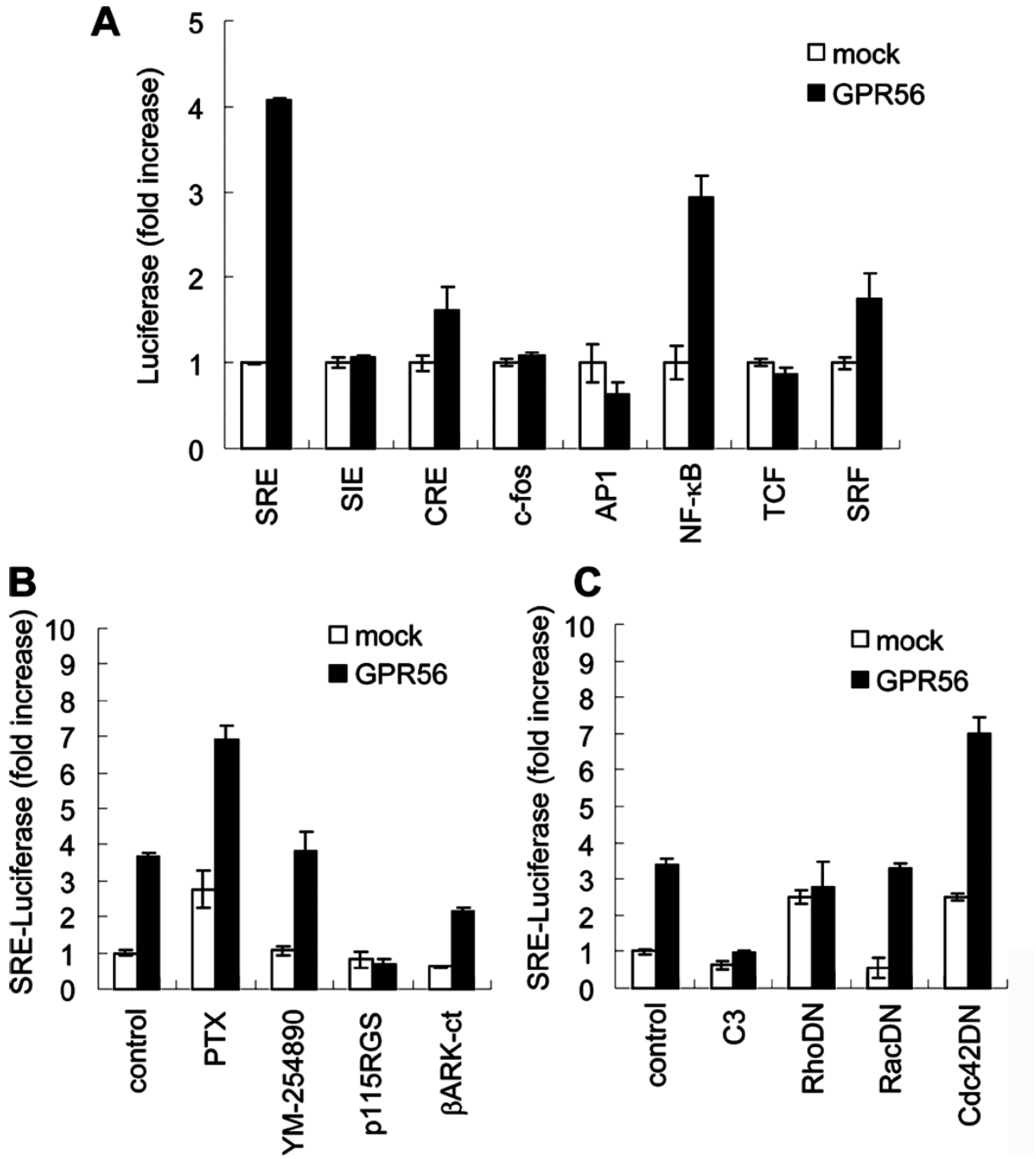

FIGURE 3. **GPR56 stimulates SRE-mediated transcription in a $G\alpha_{12/13}$- and Rho-dependent manner.** HEK293T cells were transiently transfected with an empty vector (*white bars*) or a GPR56 plasmid (*black bars*). (A) A panel of firefly luciferase reporter constructs (SRE-Luc, SIE-Luc, CRE-Luc, c-fos-Luc, AP1-Luc, NF-κB-Luc, TCF-Luc, and SRF-Luc) and a Renilla-luciferase plasmid were cotransfected with 30 ng/well empty vector or a GPR56 plasmid. (B) SRE-Luc and Renilla-Luc plasmids were co-transfected with an empty vector or GPR56 plasmids. Thirty ng/well p115 RhoGEF RGS or a βARK-ct plasmid was co-transfected. Cells were treated with pertussis toxin (PTX; 1 μg/ml) or YM-254890 (10 μM) from 1 h after transfection. (C) SRE-Luc and Renilla-Luc plasmids were co-transfected with the indicated combinations of a 30 ng/well empty vector, GPR56, C3, and 1.5 ng/well dominant negative mutants of RhoA, Rac1, or Cdc42. (A–C) Luciferase assays were carried out as described under "Experimental Procedures." The bar graph represents fold increase of SRE-luciferase activity as compared with that of empty vector-transfected cells (*error bars,* ±S.D.). All results shown are the average of triplicate samples and are representative of at least three separate experiments.

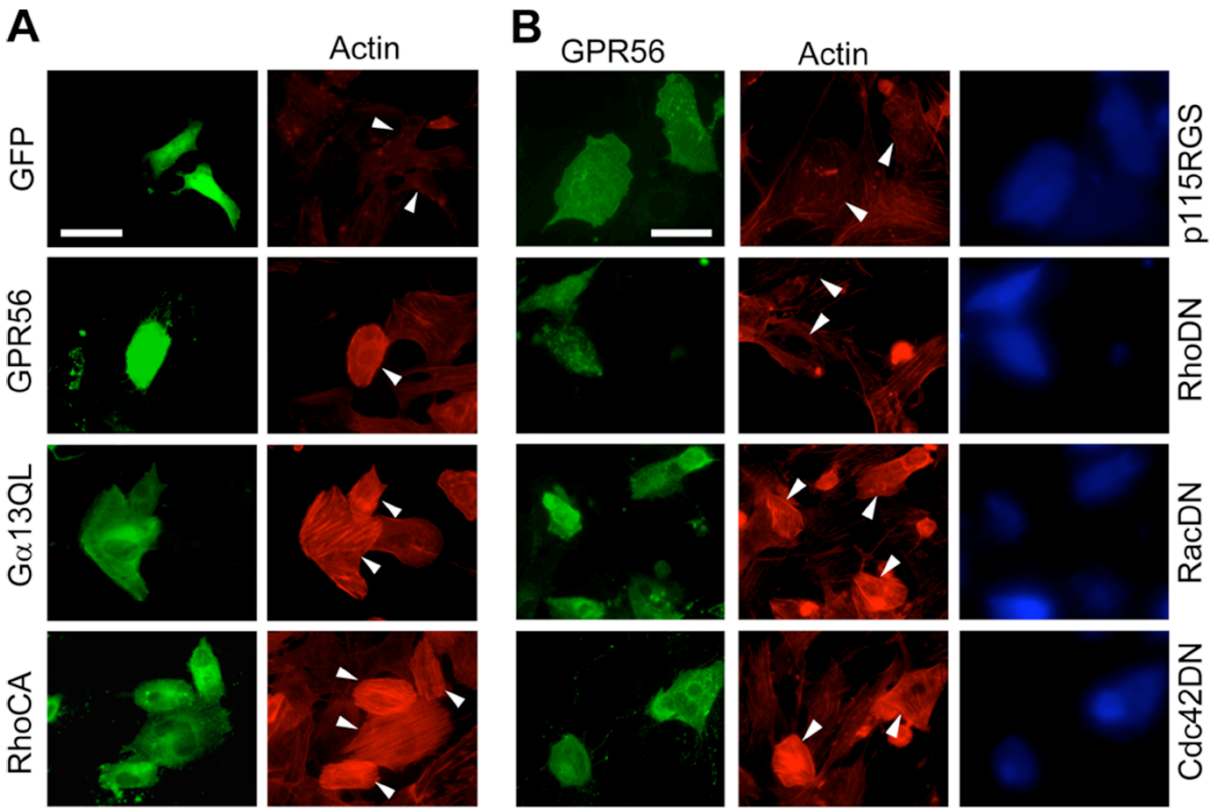

FIGURE 4. **GPR56 induces F-actin accumulation in NIH3T3 cells.** NIH3T3 cells were transfected with expression vectors harboring GPR56, $G\alpha_{13}QL$, RhoCA, and GFP (A) or a combination of GPR56 and FLAG-tagged p115 RhoGEF RGS, RhoDN, RacDN, or Cdc42DN (B). Sixteen hours after transfection, cells were starved for 6 h and then fixed and stained with Alexa-594 phalloidin (red), anti-FLAG antibody (green, $G\alpha_{13}QL$ and RhoCA; blue, p115 RhoGEF RGS, RhoDN, RacDN, and Cdc42DN), and anti-GPR56 antibody (green). The arrowheads indicate the transfected cells. *Bar*, 50 μm.

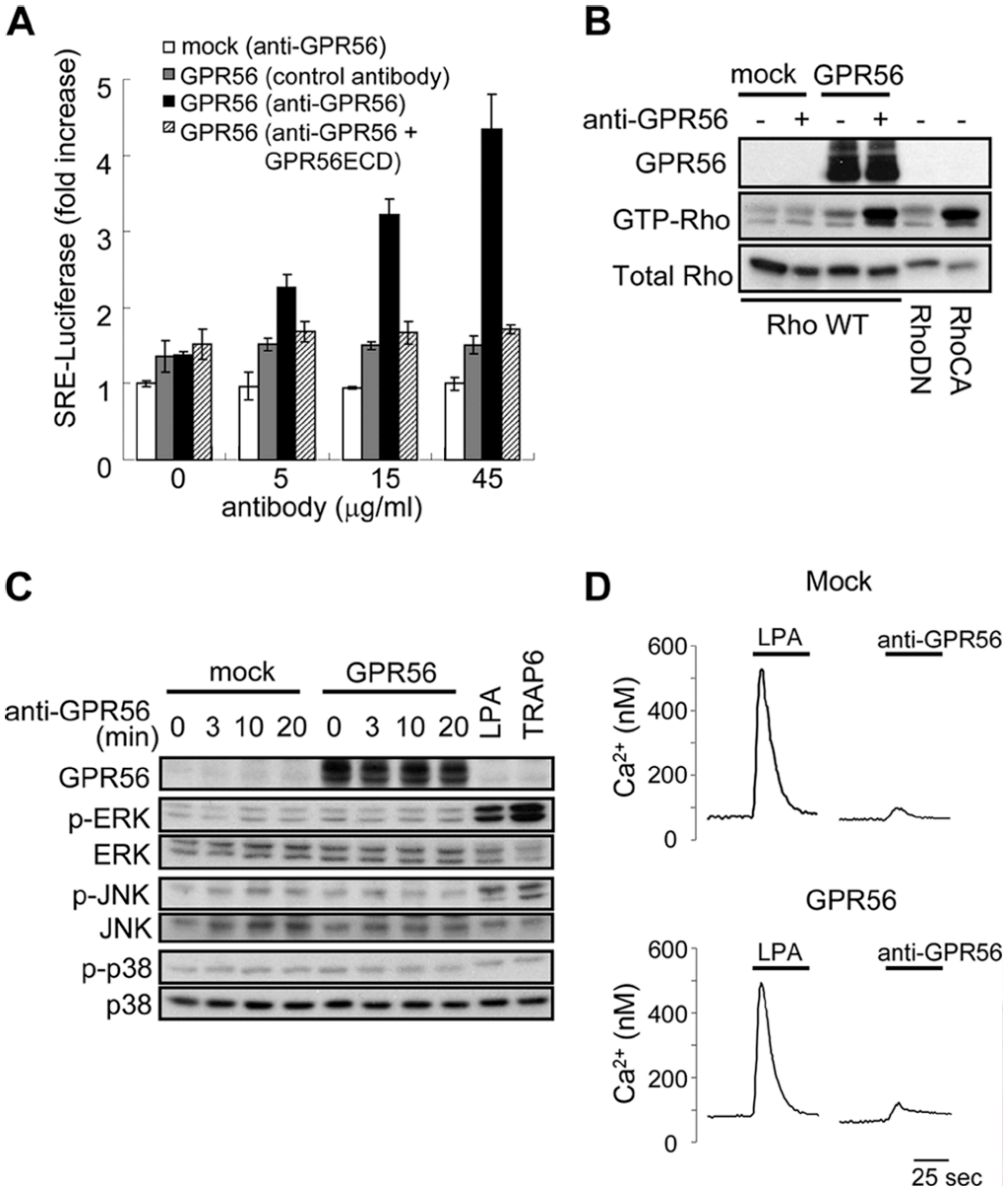

FIGURE 5. **Anti-GPR56 antibody has an agonistic activity and induces GPR56-dependent Rho activation. (**A) HEK293T cells were co-transfected with SRE-luciferase, Renilla-luciferase plasmids, and either 9 ng/well empty vector (mock) or GPR56 plasmids. Sixteen hours after transfection, a control antibody and an anti-GPR56 antibody with or without GPR56ECD (45 μg/ml) were added to the medium at the indicated concentration. The next day, cell lysates were prepared, and a luciferase assay was carried out as described under "Experimental Procedures." The bar graph represents -fold increase of normalized SRE-luciferase activity as compared with that of empty vector transfected cells without antibody stimulation (*error bars,* ±S.D.). (B) HEK293T cells were co-transfected with FLAG-RhoA, RhoDN, RhoCA, and GPR56 plasmids. The cells were stimulated with or without anti-GPR56 antibody (15 μg/ml) for 10 min. The GTP-bound form of Rho was measured by a pulldown assay using GST-mDia1RBD. Expression of RhoA in the cell lysates was estimated by immunoblotting. *WT*, wild type. (C) HEK293T cells were transfected with or without GPR56 plasmid. The cells were stimulated with anti-GPR56 antibody (15 μg/ml) for the indicated times: LPA (1 μM) for 20 min, and TRAP6 (10 μM) for 20 min. Phosphorylated MAPKs were detected by antibodies against each phospho-MAPK. (D) cells transfected with or without GPR56 plasmid were treated with LPA (1 μM) or anti-GPR56 antibody (7.5 μg/ml). Changes in intracellular free calcium were monitored using a fluorescence spectrophotometer.

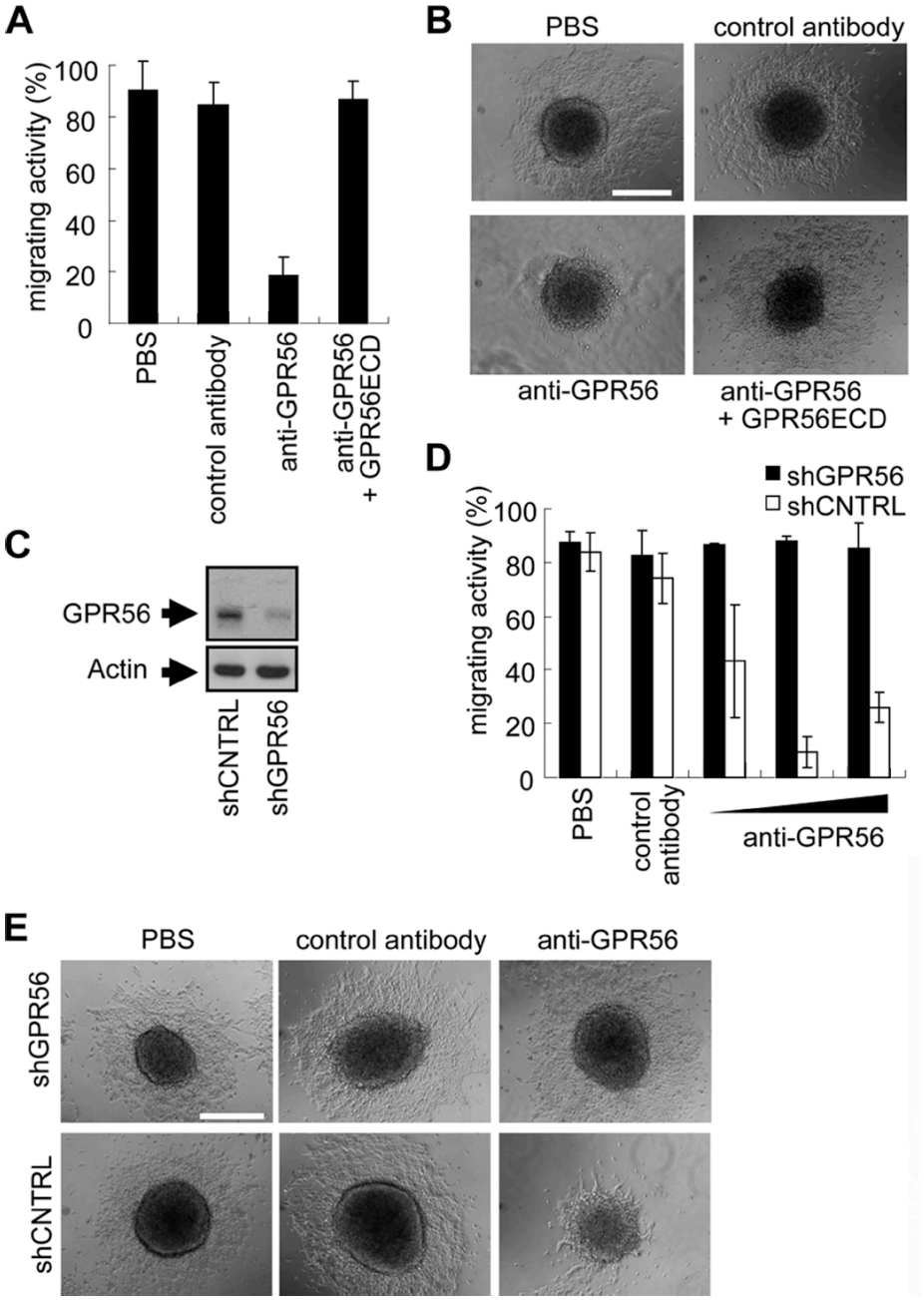

FIGURE 6. **Inhibition of NPC migration by anti-GPR56 antibody requires GPR56 expression.** (A) neurospheres were cultured for 3 days and plated on a 96-well dish coated with PEI. Plated neurospheres were cultured for 24 h in a differentiation medium containing the control antibody (15 μg/ml) or the anti-GPR56 antibody (15 μg/ml) with or without GPR56ECD (15 μg/ml). The effect of the anti-GPR56 antibody on the migration of NPCs was assessed as a percentage of the migrating neurospheres (*error bars*, ±S.D.). (B) Representative phase-contrast images are shown. (C) Neural progenitor cells were infected with an adenovirus harboring shCNTL or shGPR56 at a multiplicity of infection of 2. The knockdown efficiency in the adenovirus-infected neurospheres was detected by immunoblotting with anti-GPR56 and anti-actin antibodies. (D) Neurospheres were cultured as described in (A). Plated neurosphere were cultured in a differentiation medium containing the control antibody (11.25 μg/ml) or an anti-GPR56 antibody (3.75, 7.5, and 11.25 μg/ml). The migration of NPCs was quantified as a percentage of the migrating neurospheres (*error bars*, ±S.D.). (E) Representative phase-contrast images are shown (11.25 μg/ml control antibody and anti-GPR56 antibody). The data shown are the average of triplicate samples (A and D) and are representative (B, C, and E) of at least three separate experiments. *Bar*, 250 μm.

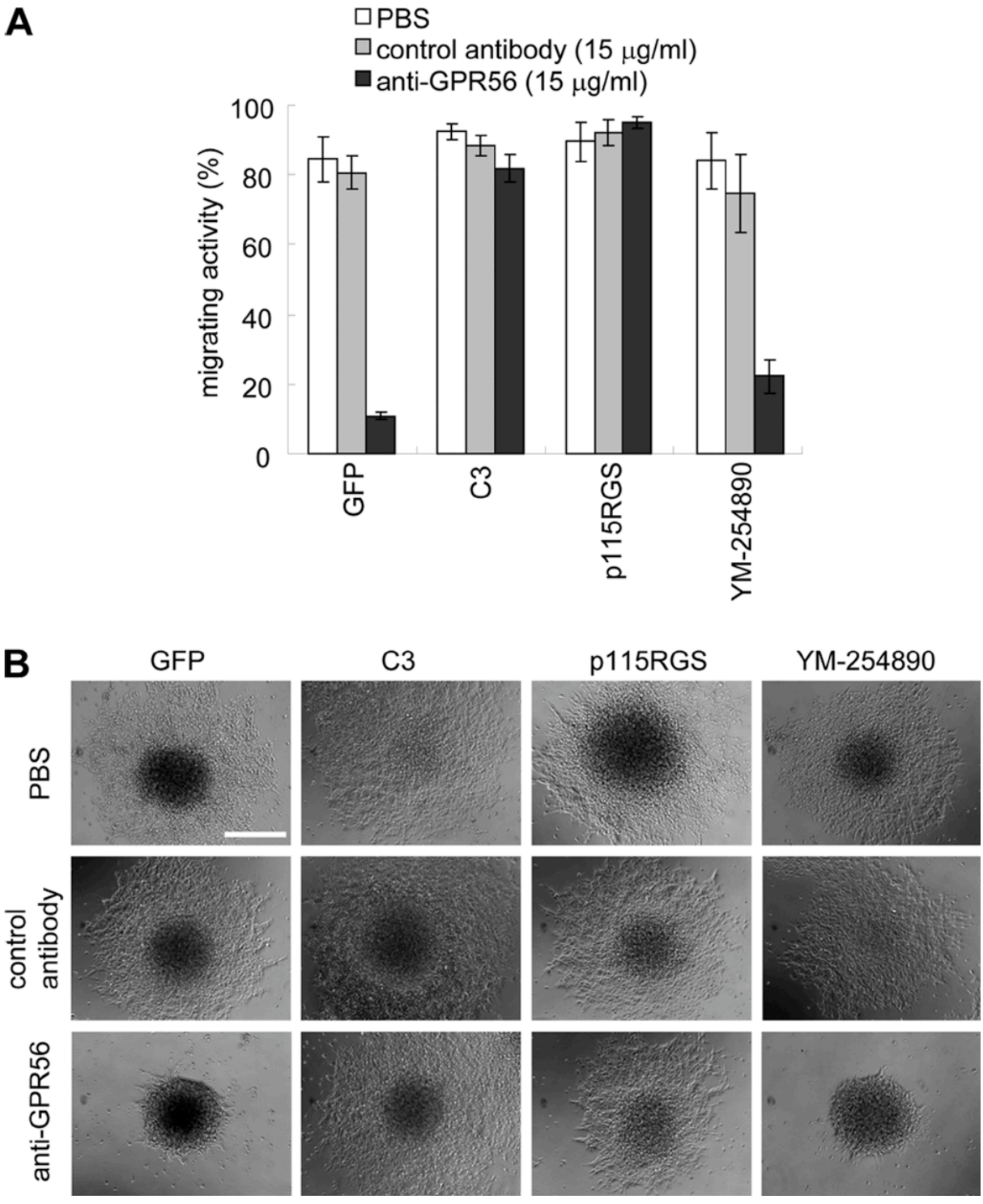

FIGURE 7. **GPR56 signal negatively regulates NPC migration through $G\alpha_{12/13}$ and Rho.** (A) Neural progenitor cells were infected with an adenovirus harboring GFP, p115 RhoGEF RGS, and C3 exoenzyme at a multiplicity of infection of 5. They were cultured under an undifferentiated condition to generate the neurosphere. Seventy-two hours after infection, neurospheres were plated on a 96-well dish coated with PEI and cultured for 24 h with a control antibody (15 μg/ml) or an anti-GPR56 antibody (15 μg/ml). YM-254890 was used at a concentration of 1 μM. The migration of NPCs was quantified as a percentage of the migrating neurospheres (error bars, ±S.D.). **(**B) Representative phase-contrast images are shown. The data shown are the average of triplicate samples (A) and are representative of at least three separate experiments (B). *Bar,* 250 μm.

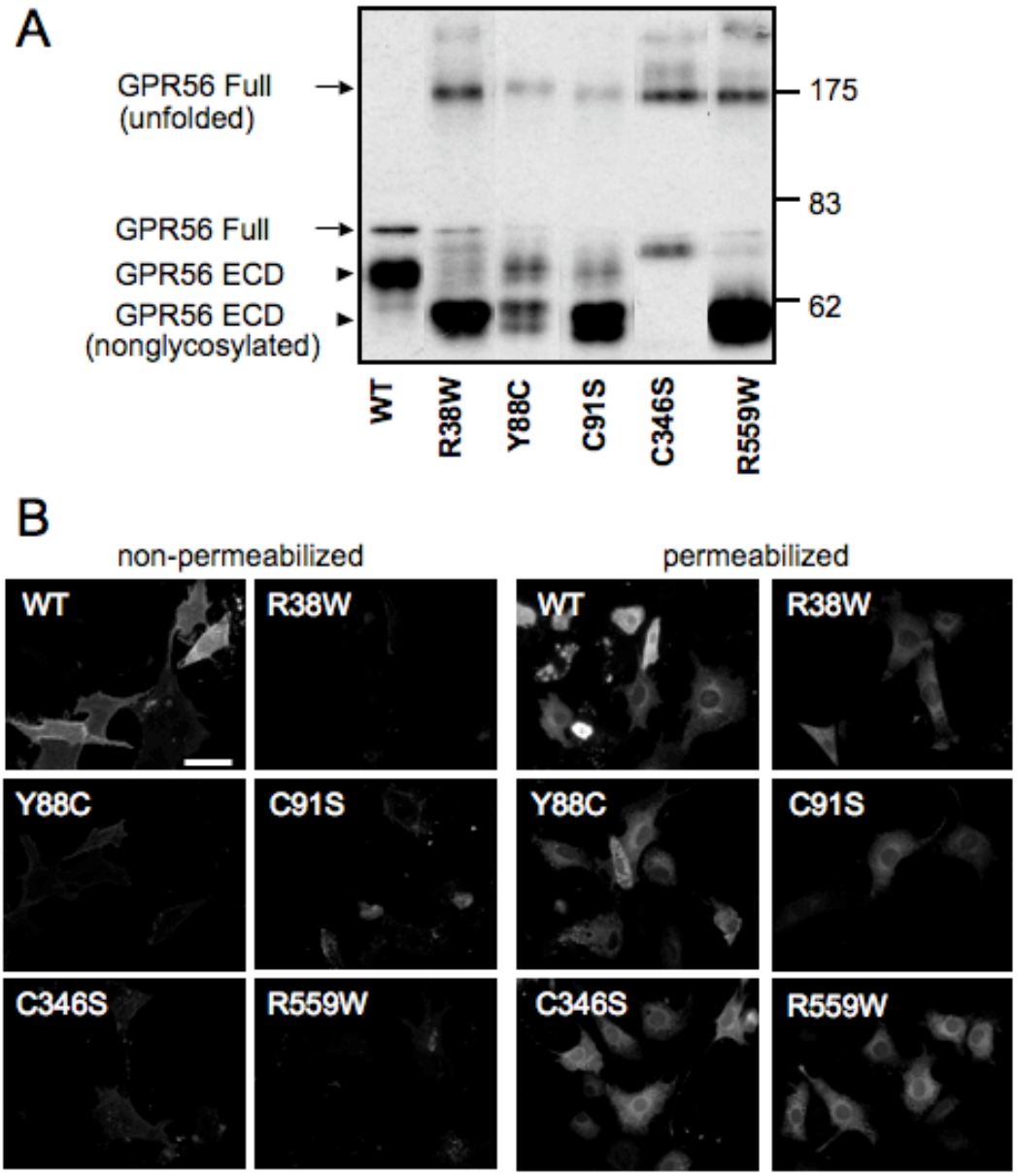

FIGURE 8. **BFPP-associated Mutations of GPR56 Affect Post-translational Modification and Cell Surface Expression. (**A) HEK293T cells were transfected with wild type GPR56 or each mutant, R38W, Y88C, C91S, C346S and R559W. Cells were lysed 48 h after transfection, and GPR56 was detected by immunoblotting. Full length of receptor (GPR56Full, *arrow*) and extracellular domain of receptor (GPR56ECD, *arrowhead*) were detected. Nonglycosylated GPR56ECD (*lower arrowhead*) was detected in the cells transfected with R38W, Y88C, C91S, and R559W. Unfolded GPR56Full (*upper arrow*) was detected in the cells transfected with all mutants. (B) Cell surface expression of receptor was assessed by immunostaining under the non-permeabilized and permeabilized condition. HEK293T cells were transiently transfected with wild type and each mutants of GPR56, then, cells were immunostained by anti-GPR56 antibody with or without detergent. Reduced surface expression was detected in the cells transfected with each mutans as compared with wild type, although receptors were expressed inside of the cell. *Bar*, 50 μm.

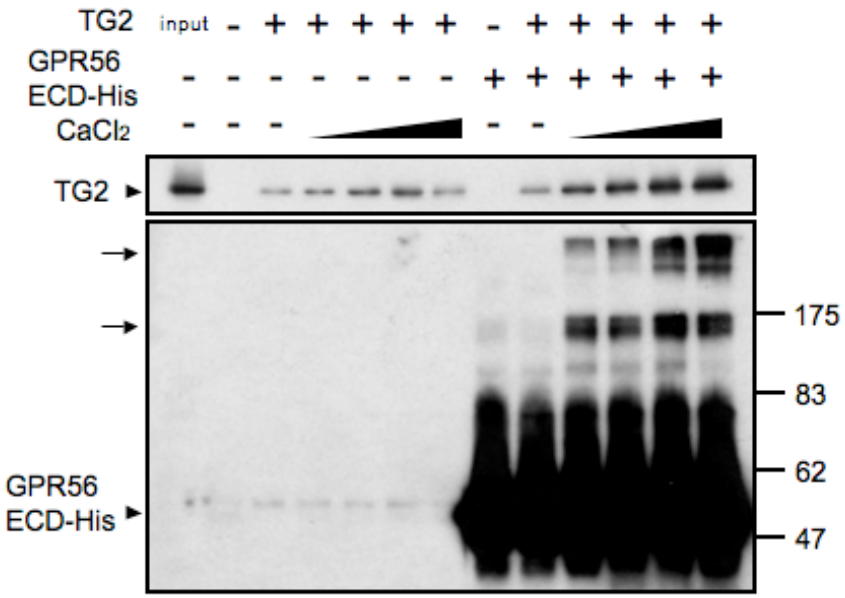

FIGURE 9. **TG2 Directly Binds to GPR56ECD in a Calcium Dependent Manner.** Recombinant TG2 (50 nM) was pulled down by hexahistidine-tagged GPR56ECD (100 nM) which was immobilized to Ni-NTA agarose at various concentrations of $CaCl_2$ (0, 1, 5, 10 and 20 mM). 10% input was used for estimation of amount of TG2. TG2 and GPR56ECD were detected by immunoblotting. Putative crosslinked GPR56ECD was indicated (*arrow*).

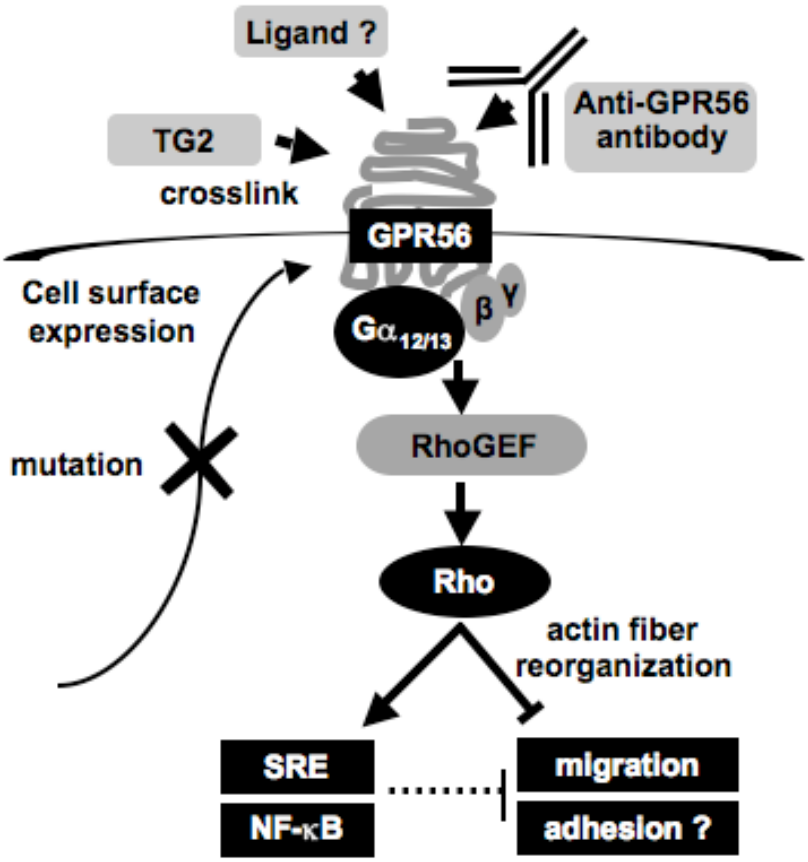

FIGURE 10. **Schematic model for the GPR56 signaling pathway that negatively regulates NPC migration.** BFPP-associated mutations of GPR56 affect cell surface expression. GPR56 stimulates actin reorganization and SRE- and NF-κB-mediated transcription in a $G\alpha_{12/13}$- and Rho-dependent manner. NPC migration is negatively regulated through the signaling pathway. Details are given under "Discussion."

Discussion

GPR56 was identified as a cortical development-associated gene in which mutations were found in patients with BFPP (27). In this disorder, the organization of the frontal cortex is disrupted, and the cortex shows thinner cortical layers and numerous small folds. GPR56 mRNA localizes in the cerebral cortical ventricular and subventricular zones during periods of neurogenesis, suggesting that the GPR56 protein is expressed in neuronal progenitors and is essential for proper lamination during brain development (27). In this study, I affinity purified antibody against GPR56 and detected high expression of GPR56 in NPCs (Fig. 1). Moreover, I showed that the overexpression of GPR56 and the agonistic antibody against GPR56 inhibited NPC migration in vitro (Figs. 2 and 6). My findings offer evidence, for the first time, of the function of GPR56 in NPCs. The inhibitory effect of GPR56 on NPC migration may be involved in brain development. Some reports have indicated the inhibitory signals of radial migration. At the end of radial migration in the cortical plate, NPCs appropriately stop their movement by the terminal signal. Reelin is well known to be a stop-signaling molecule, in which mutation causes inverted cortex lamination. Recent time lapse imaging studies on developing neocortex revealed three modes of radial migration: somal translocation; cellular locomotion; and a new mode, multipolar migration (45, 46). In this new mode of radial migration, migrating cells reduce their migration rate and change their morphology with a highly multipolar shape in the intermediate zone. On the other hand, NPCs were retained in the ventricular zone, in which neural stem cells proliferate to generate themselves and progenitors. These reduced and stop motions in radial migration appear to be an important process for the proper lamination of the cerebral cortex.

I have demonstrated that GPR56 is expressed in either a cleaved form or an uncleaved

form depending on tissue and brain development (Fig. 1, A and B). To investigate whether the truncated GPR56 is active and whether the cleaved GPR56ECD acts as an agonist itself, I constructed the truncated mutant that has a FLAG tag instead of the amino acid sequence from Asp-94 to Leu-382. However, the truncated mutant failed to be expressed in the cell surface (data not shown). I constructed the five BFPP-associated mutants of GPR56, and investigated the effect of these mutations on GPR56 function. From the immunoblotting analysis, I revealed that the mutations of GPR56 defected proper folding of receptor and caused reduced glycosylation at the extracellular domain. These miss modifications resulted in the reduced expression of receptor in the cell surface (Fig. 8). These results are consistent with recent study (28), which also indicated the impairment of cell surface expression caused by mutations. All mutations of GPR56 in BFPP patients sited in the regions that face outside of the cell. Therefore, the impairment of receptor to bind to the ligands was thought to be the only reason for BFPP. However, I and other group (28) revealed that posttranslational processing of GPR56 in the N-terminal region is important for cell surface expression. It should be a reason why the mutations of GPR56 cause a cortical malformation.. Anyway, the details of the activation mechanism of GPR56 remain to be clarified.

Defective cell surface expression of GPR56 may result in the impairment of binding to its ligand. I showed that GPR56 knockdown did not affect NPC migration, whereas GPR56 overexpression inhibited the migration. These results suggested that my in vitro migration assay might lack a ligand for GPR56. GPR56 may be activated in the developmental forebrain at the proper place where a ligand of GPR56 exists. Thus, the mutation of GPR56 may cause cortical malformation by its impairment of the ability to bind to the stop signal molecules. Recently, tissue transglutaminase 2 (TG2) was reported as the candidate ligand of GPR56 (32). TG2 is an extracellular matrix protein expressed ubiquitously in tissues and

organs and functions as a cross-linking enzyme in the matrix (47). I investigated the whether TG2 functions as a ligand of GPR56. I demonstrated that TG2 directly binds to GPR56ECD in a calcium dependent manner. Moreover in the presence of TG2 and calcium, GPR56ECD was detected as the high molecular weight bands (Fig. 9). These results might be caused by crosslinking of GPR56ECD, because TG2 catalyzes Ca^{2+} dependent protein crosslinking (47). I also investigated the effect of TG2 on the GPR56 signaling. However, the co-expression of TG2 did not stimulate GPR56-dependent SRE-mediated transcriptional activation (data not shown). It might be needed to carry out the assay in which TG2 is added from the outoside of the cells. It remains to be cralified whether TG2 might work as a ligand or as a modulator of ligand binding with GPR56. Finding a ligand for GPR56 or elucidating the activation mechanism of GPR56 will be necessary for understanding the proper lamination of the cortical brain.

I next investigated the signaling pathway that is mediated through GPR56. The signaling pathways of the adhesion GPCR family, including GPR56, are largely unknown, because most of the members are orphan receptors. I utilized two effective approaches to reveal the signaling pathway. First, I examined the effect of GPR56 overexpression on the activation of transcription factors using firefly luciferase reporter genes. The overexpression of GPCR can stimulate ligand-independent signal activation by increasing the active form, which is bound to GTP in a multistate conversion model of GPCR (40). It has been reported that the overexpression of G2A, a member of GPCR, elicits the activation of G protein signaling (41). I have shown here that GPR56 induces $G\alpha_{12/13}$- and Rho-dependent activation of transcription mediated through the SRE and NF-κB- responsive element in HEK293T cells (Fig. 3). Moreover, actin stress fibers in NIH3T3 cells were reorganized by the overexpression of GPR56 in a $G\alpha_{12/13}$- and Rho-dependent manner (Fig. 4). Previously, Shashidhar et al. (31) reported that GPR56 overexpression in 293 cells activated the TCF,

the PAI-1, and, to a lesser extent, the NF-κB-responsive element, using a β-galactosidase reporter assay. They also indicated a slight activation of SRE in GPR56-overexpressing cells. However, these activation mechanisms have not yet been described elsewhere.

Second, I was able to prepare the agonistic antibody which functions as a ligand for GPR56. Some antibodies against the extracellular region of GPCR can be used instead of ligands to stimulate the receptor. For example, the antibodies directed to the second extracellular loop of M2R are known to work as a partial agonist (42). Constitutive activation of the thyroid-stimulating hormone receptor (TSHR) in Grave disease is widely acknowledged to be caused by an antibody-mediated autoimmune reaction (43). I showed that the anti-GPR56 antibody induced SRE-mediated transcription with Rho activation and inhibited NPC migration. Neutralization with antigen GPR56ECD completely blocked anti-GPR56 antibody-induced SRE activation (Fig. 5A) and inhibition of NPC migration (Fig. 6, A and B). GPR56 knockdown also attenuated the inhibitory effect of the anti-GPR56 antibody on NPC migration (Fig. 6,D and E). These results supported the idea that the anti-GPR56 antibody prepared in this study specifically stimulated GPR56 activity. So, what is the mechanism in which anti-GPR56 antibody stimulates GPR56? TSH receptor that also has a large extracellular N-teminal region, which is divided into N-terminal ectodomain and rest of the seven transmembrane regions of TSH receptor, might be the model of GPR56 activation. TSHR is usually kept inactive state by the N-terminal ectodomain. Upon binding of TSH, ectodomain is swiched from antagonist to agonist. Crystal structure of the TSHR complex with a thyroid-stimulating autoantibody revealed that autoantibody against TSHR also activates the receptor as a same manner (48). Therefore, the elucidation of the interaction face of antibody to the extracellualr region of GPR56 might help the understanding the activation mechanism of GPR56 by the ligand.

The $G\alpha_{12}$ family of heterotrimeric G proteins, consisting of $G\alpha_{12}$ and $G\alpha_{13}$, regulates

various cellular responses through small GTPase Rho. These responses include the activation of SRE and actin stress fiber formation. Therefore, I thought that GPR56 should be coupled with the $G\alpha_{12}$ family of heterotrimeric G proteins. I demonstrated that p115 RhoGEF RGS, a specific inhibitory molecule of $G\alpha_{12/13}$, blocked SRE activation (Fig. 3B) and actin fiber formation (Fig. 4B) by GPR56 overexpression and the inhibitory effect on NPC migration by the anti-GPR56 antibody (Fig. 7). The C3 exoenzyme, which specifically inhibits Rho by ADP-ribosylation, also attenuated SRE activation and the inhibition of NPC migration (Figs. 3C and 7). These results indicate that GPR56 has the ability to transduce signals through $G\alpha_{12/13}$ and Rho in various cells and to inhibit NPC migration (Fig. 10). A recent study indicated the importance of $G\alpha_{12/13}$ and Rho signaling in neural cell morphology and cortical development. Fukushima *et al*. (49) reported that LPA induces the contraction of neuroblast clusters through Rho-dependent actin polymerization, which is involved in the cell rounding of interkinetic nuclear migration. LPA is known to activate Rho through $G\alpha_{12/13}$. More recently, Moers *et al*. (50) reported that conditional knock-out of the $G\alpha_{12}$ and $G\alpha_{13}$ in the nervous system causes localized overmigration of neurons in the developing cerebral and cerebellar cortices. Therefore, these reports may provide a basis for understanding the mechanisms whereby the activation of GPR56 inhibits the spread of NPCs from the neurosphere and regulates cortical development. GPR56 might regulate NPC behavior by changing the cell morphology through the actin reorganization in the cerebral cortex.

Little *et al.* (51) reported that GPR56 physically associates with $G\alpha_{q/11}$ in the complex of tetraspanins CD81 and CD9, which are small membrane proteins involved in the regulation of cell migration and mitotic activity. It has been reported that CD81 is expressed in neural progenitor cells and that CD81- null mouse shows an increase in brain size and glial cell number, suggesting that CD81 is involved in the development of the central nervous system

(52). However, in my experiments, the inhibition of $G\alpha_{q/11}$ by YM-254890 did not affect the activation of SRE and inhibition of NPC migration induced by GPR56. Moreover, GPR56-mediated intracellular Ca^{2+} mobilization was not observed (Fig. 5D). GPR56 might transduce the signals through different Gα subunits in a cell- and tissue-specific manner. Previously, Mizuno et al. (20) demonstrated that $G\alpha_q$- and JNK-mediated signals inhibit NPC migration and may be involved in the multipolar migration at the intermediate zone of the cortical layer. I have now indicated that GPR56 signaling via $G\alpha_{12/13}$ and Rho negatively regulates NPC migration. The inhibitory effects of $G\alpha_{q/11}$ and $G\alpha_{12/13}$ may be regulated by distinct mechanisms, because GPR56 signaling did not inhibit neural progenitor cell migration in a laminin-coated dish, whereas endothelin receptor signaling via $G\alpha_{q/11}$ and JNK did so, independently of Rho. Because GPR56 is highly expressed in the ventricular zone of the cortical layer (Fig. 1D, VZ), the inhibitory regulation of NPC migration by GPR56 might be essential for the retention of NPCs at the ventricular zone. BFPP brain shows abnormally numerous and small gyri caused by disruption of the normal six layer into only four layers (27). Disfunction of GPR56 might cause the unregulated start of NPC migration, in which NPCs are not mature for construction of the targetted layer. The thin layer of BFPP brain might be caused by the reduction of the neural stem cells which should be retained and proliferate the cells that is necessary for construction of the brain. It would be of interest to investigate the cortical development of GPR56 knock-out mouse and cortical slice cultures in which GPR56 is knocked down. Further research on GPR56 and the identification of the ligand for GPR56 should provide a better understanding of the role of GPCR signaling in brain development.

Acknowledgements

I would like to thank Director Professor Hiroshi Itoh for his suggestion and discussion throughout my study. I acknowledge Dr. Naoyuki Inagaki, Dr. Norikazu Mizuno, Dr. Kenji Tago and Dr. Tadayuki Shimada for their helpful discussions and encouragement. I thank Dr. Sadao Shiosaka for various advices, Dr. Hitoshi Kurose (Kyushyu University) for the gift of the adenovirus, and Dr. Jun Takasaki (Astellas Pharma Inc.) for the gift of YM-254890. I also thank all current and previous members of the Itoh laboratory for helpful discussions.

References

1. Marin, O., and Rubenstein, J. L. (2003). Cell migration in the forebrain. *Annu. Rev. Neurosci.* **26**, 441-483.
2. Bielas, S., Higginbotham, H., Koizumi, H., Tanaka, T., and Gleeson, J. G. (2004). Cortical neuronal migration mutants suggest separate but intersecting pathways. *Annu. Rev. Cell Dev. Biol.* **20**, 593-618.
3. Marin, O., Valdeolmillos, M., and Moya, F. (2006). Neurons in motion: same principles for different shapes? *Trends Neurosci.* **29**, 655-661.
4. D'Arcangelo, G., Miao, G. G., Chen, S. C., Soares, H. D., Morgan, J. I., and Curran, T. (1995). A protein related to extracellular matrix proteins deleted in the mouse mutant reeler. *Nature* **374**, 719-723.
5. Hirotsune, S., Takahara, T., Sasaki, N., Hirose, K., Yoshiki, A., Ohashi, T., Kusakabe, M., Murakami, Y., Muramatsu, M., and Watanabe, S. (1995). The reeler gene encodes a protein with an EGF-like motif expressed by pioneer neurons. *Nat. Genet.* **10**, 77-83.
6. Ogawa, M., Miyata, T., Nakajima, K., Yagyu, K., Seike, M., Ikenaka, K., Yamamoto, H., and Mikoshiba, K. (1995). The reeler gene-associated antigen on Cajal-Retzius neurons is a crucial molecule for laminar organization of cortical neurons. *Neuron* **14**, 899-912.
7. Reiner, O., Carrozzo, R., Shen, Y., Wehnert, M., Faustinella, F., Dobyns, W. B., Caskey, C. T., and Ledbetter, D. H. (1993). Isolation of a Miller-Dieker lissencephaly gene containing G protein beta-subunit-like repeats. *Nature* **364**, 717-721.
8. Hattori, M., Adachi, H., Tsujimoto, M., Arai, H., and Inoue, K. (1994). Miller-Dieker lissencephaly gene encodes a subunit of brain platelet-activating factor. *Nature* **370**, 216-218.
9. des Portes, V., Pinard, J. M., Billuart, P., Vinet, M. C., Koulakoff, A., Carrie, A., Gelot,

A., Dupuis, E., Motte, J., Berwald-Netter, Y., Catala, M., Kahn, A., Beldjord, C., and Chelly, J. (1998). A novel CNS gene required for neuronal migration and involved in X-linked subcortical laminar heterotopia and lissencephaly syndrome. *Cell* **92**, 51-61.

10. Gleeson, J. G., Allen, K. M., Fox, J. W., Lamperti, E. D., Berkovic, S., Scheffer, I., Cooper, E. C., Dobyns, W. B., Minnerath, S. R., Ross, M. E., and Walsh, C. A. (1998). Doublecortin, a brain-specific gene mutated in human X-linked lissencephaly and double cortex syndrome, encodes a putative signaling protein. *Cell* **92**, 63-72.
11. Etienne-Manneville, S., and Hall, A. (2002). Rho GTPases in cell biology. *Nature* **420**, 629-635.
12. Kholmanskikh, S. S., Dobrin, J. S., Wynshaw-Boris, A., Letourneau, P. C., and Ross, M. E. (2003). Disregulated RhoGTPases and actin cytoskeleton contribute to the migration defect in Lis1-deficient neurons. *J. Neurosci.* **23**, 8673-8681.
13. Gilman, A. G. (1987). G proteins: transducers of receptor-generated signals. *Annu. Rev. Biochem.* **56**, 615-649.
14. Marinissen, M. J., and Gutkind, J. S. (2001). G-protein-coupled receptors and signaling networks: emerging paradigms. *Trends Pharmacol. Sci.* **22**, 368-376.
15. Kaziro, Y., Itoh, H., Kozasa, T., Nakafuku, M., and Satoh, T. (1991). Structure and function of signal-transducing GTP-binding proteins. *Annu. Rev. Biochem.* **60**, 349-400.
16. Milligan, G., and Kostenis, E. (2006). Heterotrimeric G-proteins: a short history. *Br. J. Pharmacol.* **147 Suppl 1**, S46-55.
17. Behar, T. N., Schaffner, A. E., Scott, C. A., Greene, C. L., and Barker, J. L. (2000). GABA receptor antagonists modulate postmitotic cell migration in slice cultures of embryonic rat cortex. *Cereb. Cortex* **10**, 899-909.
18. Behar, T. N., Smith, S. V., Kennedy, R. T., McKenzie, J. M., Maric, I., and Barker, J. L. (2001). GABA(B) receptors mediate motility signals for migrating embryonic cortical

cells. *Cereb. Cortex* **11**, 744-753.

19. Stumm, R. K., Zhou, C., Ara, T., Lazarini, F., Dubois-Dalcq, M., Nagasawa, T., Hollt, V., and Schulz, S. (2003). CXCR4 regulates interneuron migration in the developing neocortex. *J. Neurosci.* **23**, 5123-5130.
20. Mizuno, N., Kokubu, H., Sato, M., Nishimura, A., Yamauchi, J., Kurose, H., and Itoh, H. (2005). G protein-coupled receptor signaling through Gq and JNK negatively regulates neural progenitor cell migration. *Proc. Natl. Acad. Sci. U. S. A.* **102**, 12365-12370.
21. Shinohara, H., Udagawa, J., Morishita, R., Ueda, H., Otani, H., Semba, R., Kato, K., and Asano, T. (2004). Gi2 signaling enhances proliferation of neural progenitor cells in the developing brain. *J. Biol. Chem.* **279**, 41141-41148.
22. Liu, M., Parker, R. M., Darby, K., Eyre, H. J., Copeland, N. G., Crawford, J., Gilbert, D. J., Sutherland, G. R., Jenkins, N. A., and Herzog, H. (1999). GPR56, a novel secretin-like human G-protein-coupled receptor gene. *Genomics* **55**, 296-305.
23. Fredriksson, R., Lagerstrom, M. C., Hoglund, P. J., and Schioth, H. B. (2002). Novel human G protein-coupled receptors with long N-terminals containing GPS domains and Ser/Thr-rich regions. *FEBS Lett.* **531**, 407-414.
24. Fredriksson, R., Gloriam, D. E., Hoglund, P. J., Lagerstrom, M. C., and Schioth, H. B. (2003). There exist at least 30 human G-protein-coupled receptors with long Ser/Thr-rich N-termini. *Biochem. Biophys. Res. Commun.* **301**, 725-734.
25. Bjarnadottir, T. K., Fredriksson, R., Hoglund, P. J., Gloriam, D. E., Lagerstrom, M. C., and Schioth, H. B. (2004). The human and mouse repertoire of the adhesion family of G-protein-coupled receptors. *Genomics* **84**, 23-33.
26. Bjarnadottir, T. K., Fredriksson, R., and Schioth, H. B. (2007). The Adhesion GPCRs: A unique family of G protein-coupled receptors with important roles in both central and

peripheral tissues. *Cell Mol. Life Sci.* **64**, 2104-2119.

27. Piao, X., Hill, R. S., Bodell, A., Chang, B. S., Basel-Vanagaite, L., Straussberg, R., Dobyns, W. B., Qasrawi, B., Winter, R. M., Innes, A. M., Voit, T., Ross, M. E., Michaud, J. L., Descarie, J. C., Barkovich, A. J., and Walsh, C. A. (2004). G protein-coupled receptor-dependent development of human frontal cortex. *Science* **303**, 2033-2036.

28. Jin, Z., Tietjen, I., Bu, L., Liu-Yesucevitz, L., Gaur, S. K., Walsh, C. A., and Piao, X. (2007). Disease-associated Mutations Affect GPR56 Protein Trafficking and Cell Surface Expression. *Hum. Mol. Genet.* **16,** 1972-1985.

29. Terskikh, A. V., Easterday, M. C., Li, L., Hood, L., Kornblum, H. I., Geschwind, D. H., and Weissman, I. L. (2001). From hematopoiesis to neuropoiesis: evidence of overlapping genetic programs. *Proc. Natl. Acad. Sci. U. S. A.* **98**, 7934-7939.

30. Zendman, A. J., Cornelissen, I. M., Weidle, U. H., Ruiter, D. J., and van Muijen, G. N. (1999). TM7XN1, a novel human EGF-TM7-like cDNA, detected with mRNA differential display using human melanoma cell lines with different metastatic potential. *FEBS Lett.* **446**, 292-298.

31. Shashidhar, S., Lorente, G., Nagavarapu, U., Nelson, A., Kuo, J., Cummins, J., Nikolich, K., Urfer, R., and Foehr, E. D. (2005). GPR56 is a GPCR that is overexpressed in gliomas and functions in tumor cell adhesion. *Oncogene* **24**, 1673-1682.

32. Xu, L., Begum, S., Hearn, J. D., and Hynes, R. O. (2006). GPR56, an atypical G protein-coupled receptor, binds tissue transglutaminase, TG2, and inhibits melanoma tumor growth and metastasis. *Proc. Natl. Acad. Sci. U. S. A.* **103**, 9023-9028.

33. Sud, N., Sharma, R., Ray, R., Chattopadhyay, T. K., and Ralhan, R. (2006). Differential expression of G-protein coupled receptor 56 in human esophageal squamous cell carcinoma. *Cancer Lett.* **233**, 265-270.

34. Ke, N., Sundaram, R., Liu, G., Chionis, J., Fan, W., Rogers, C., Awad, T., Grifman, M.,

Yu, D., Wong-Staal, F., and Li, Q. X. (2007). Orphan G protein-coupled receptor GPR56 plays a role in cell transformation and tumorigenesis involving the cell adhesion pathway. *Mol. Cancer. Ther.* **6**, 1840-1850.

35. Arai, K., Maruyama, Y., Nishida, M., Tanabe, S., Takagahara, S., Kozasa, T., Mori, Y., Nagao, T., and Kurose, H. (2003). Differential requirement of G alpha12, G alpha13, G alphaq, and G beta gamma for endothelin-1-induced c-Jun NH2-terminal kinase and extracellular signal-regulated kinase activation. *Mol. Pharmacol.* **63**, 478-488.
36. Sun, Y., Yamauchi, J., Kaziro, Y., and Itoh, H. (1999). Activation of c-fos promoter by Gbetagamma-mediated signaling: involvement of Rho and c-Jun N-terminal kinase. *J. Biochem. (Tokyo)* **125**, 515-521.
37. Yamauchi, J., Hirasawa, A., Miyamoto, Y., Itoh, H., and Tsujimoto, G. (2001). Beta2-adrenergic receptor/cyclic adenosine monophosphate (cAMP) leads to JNK activation through Rho family small GTPases. *Biochem. Biophys. Res. Commun.* **284**, 1199-1203
38. Sakata, K. (2006). オーファンGタンパク質共役型受容体GPR56の機能解析及びリガンド探索 *A Master's Thesis, Graduate School of Biological Sciences, Nara Institute of Science and Technology.*
39. Takasaki, J., Saito, T., Taniguchi, M., Kawasaki, T., Moritani, Y., Hayashi, K., and Kobori, M. (2004). A novel Galphaq/11-selective inhibitor. *J. Biol. Chem.* **279**, 47438-47445.
40. Seifert, R., and Wenzel-Seifert, K. (2002). Constitutive activity of G-protein-coupled receptors: cause of disease and common property of wild-type receptors. *Naunyn Schmiedebergs Arch. Pharmacol.* **366**, 381-416.
41. Kabarowski, J. H., Feramisco, J. D., Le, L. Q., Gu, J. L., Luoh, S. W., Simon, M. I., and Witte, O. N. (2000). Direct genetic demonstration of G alpha 13 coupling to the orphan

G protein-coupled receptor G2A leading to RhoA-dependent actin rearrangement. *Proc. Natl. Acad. Sci. U. S. A.* **97**, 12109-12114.

42. Elies, R., Fu, L. X., Eftekhari, P., Wallukat, G., Schulze, W., Granier, C., Hjalmarson, A., and Hoebeke, J. (1998). Immunochemical and functional characterization of an agonist-like monoclonal antibody against the M2 acetylcholine receptor. *Eur. J. Biochem.* **251**, 659-666.
43. Schott, M., Scherbaum, W. A., and Morgenthaler, N. G. (2005). Thyrotropin receptor autoantibodies in Graves' disease. *Trends Endocrinol. Metab.* **16**, 243-248.
44. Makita, N., Sato, J., Manaka, K., Shoji, Y., Oishi, A., Hashimoto, M., Fujita, T., and Iiri, T. (2007). An acquired hypocalciuric hypercalcemia autoantibody induces allosteric transition among active human Ca-sensing receptor conformations. *Proc. Natl. Acad. Sci. U. S. A.* **104**, 5443-5448.
45. Tabata, H., and Nakajima, K. (2003). Multipolar migration: the third mode of radial neuronal migration in the developing cerebral cortex. *J. Neurosci.* **23**, 9996-10001.
46. Nadarajah, B., Alifragis, P., Wong, R. O., and Parnavelas, J. G. (2003). Neuronal migration in the developing cerebral cortex: observations based on real-time imaging. *Cereb. Cortex* **13**, 607-611.
47. Fesus, L., and Piacentini, M. (2002). Transglutaminase 2: an enigmatic enzyme with diverse functions. *Trends Biochem. Sci.* **27**, 534-539.
48. Sanders, J., Chirgadze, DY., Sanders, P., Baker, S., Sullivan, A., Bhardwaja, A., Bolton, J., Reeve, M., Nakatake, N., Evans, M., Richards, T., Powell, M., Miguel, RN., Blundell, TL., Furmaniak, J., Smith, BR. (2007). Crystal Structure of the TSH Receptor in Complex with a Thyroid-Stimulating Autoantibody. *Thyroid.* **17**, 395-410
49. Fukushima, N., Weiner, J. A., and Chun, J. (2000). Lysophosphatidic acid (LPA) is a novel extracellular regulator of cortical neuroblast morphology. *Dev. Biol.* **228**, 6-18.

50. Moers, A., Nurnberg, A., Goebbels, S., Wettschureck, N., and Offermans, S. (2008). Galpha12/Galpha13 deficiency causes localized overmigration of neurons in the developing cerebral and cerebellar cortices. *Mol. Cell. Biol.* **28**, 1480-1488.

51. Little, K. D., Hemler, M. E., and Stipp, C. S. (2004). Dynamic regulation of a GPCR-tetraspanin-G protein complex on intact cells: central role of CD81 in facilitating GPR56-Galpha q/11 association. *Mol. Biol. Cell* **15**, 2375-2387.

52. Geisert, E. E.,Jr, Williams, R. W., Geisert, G. R., Fan, L., Asbury, A. M., Maecker, H. T., Deng, J., and Levy, S. (2002). Increased brain size and glial cell number in CD81-null mice. *J. Comp. Neurol.* **453**, 22-32.